An All-Fiber RF Modulation Technique: Frequency Response Calibration of Optical Detectors

Jose L. Cruz, Javier Marzal, and Miguel V. Andrés

Abstract—**Two all-fiber Mach-Zender interferometers have been designed to generate RF modulated light at 633 nm and 830 nm. The interferometers are scanned with a piezoelectric tube driven at its fundamental frequency of resonance. The actual experimental arrangement covers the frequency range 1 kHz to 1 GHz. The technique combines several interesting features as the simplicity, the stability and reliability of all-fiber systems and the use of low-frequency electronics to control and generate the RF modulated light.**

I. Introduction

We present in this paper an all-fiber technique to generate a RF modulated light. The bases of the technique were presented using a Michelson and a low finesse Fabry-Perot interferometers [1]. Both interferometers were powered by a 5 mW multimode HeNe laser (633 nm) and we covered the frequency range 1 kHz to 45 MHz. We have improved those results designing a Mach Zender interferometer, being able to cover a frequency range up to 600 MHz. Furthermore, we have designed another Mach-Zender interferometer powered by a 830 nm diode laser. This system covers the frequency range 1 kHz to 1 GHz.

Our RF modulation technique was developed to calibrate the frequency response of optical detectors. The technique was proposed as an alternative to an opto-mechanical frequency response calibrator [2], designed for accurate measurements in the megahertz range. Our present results show that this technique can be used in the RF range and that it can be extended to the GHz range. In fact, the same system could be used to measure the frequency response of low-frequency and high-frequency optical detectors.

As a frequency response calibration technique, the most outstanding characteristic is its simplicity. The equipment, that is required, is probably available at any optical fiber laboratory. Other techniques like the optical heterodyne technique [3], the optical intensity noise technique [4], [5] and the time domain picosecond pulse technique [6] require either narrow-linewidth tuneable lasers or optical amplifiers or picosecond lasers, respectively. Moreover, the signal processing required is as straightforward as for other techniques [3], [4].

Since it is advisable to measure the characteristics of a detector under conditions as close as possible to those of the application, we should mention that our calibration technique can be easily implemented at any wavelength, provided that single-mode fiber and CW lasers are available. Furthermore, the detector is subjected to no high peak power and the average power can be easily adjust between zero and the maximum power supplied by the laser.

Manuscript received January 18, 1995; revised April 12, 1995. This work was supported in part by DGICYT of Spain Grant TIC93-1203 and the Institució Valenciana d'Estudis i Investigació.

The authors are with the Departamento de Física Aplicada, Universidad de Valencia, 46100 Burjasot (Valencia), Spain.

IEEE Log Number 9413688.

II. Theory

The principle of our modulation technique is to scan an optical fiber Mach-Zender interferometer, using a piezoelectric tube with a long piece of singlemode fiber wound round it. Fig. 1 gives a diagram of our experimental arrangement. Applying a voltage of low frequency, Ω, to the tube, the fiber is strained and a controlled phase change, $\Delta\Phi$, is generated

$$\Delta\Phi = \Phi_0 + \frac{1}{2}\Phi_{pp}\sin(\Omega t) \tag{1}$$

where Φ_0 is $\Delta\Phi$ at $t = 0$ and Φ_{pp} is the peak to peak amplitude modulation. The relative output of the interferometer, $P_o(t)/P_i$, can be written as

$$\frac{P_o(t)}{P_i} = \frac{1}{2}(1 - \cos(\Delta\Phi(t))). \tag{2}$$

Thus, the velocity of the phase change determines the modulation frequency of the interferometer output, one cycle corresponding to a phase change of 2π.

Substituting (1) into (2), we can worked out the frequency spectrum of the interferometer modulated output [7]

$$A_n(n\Omega) = \begin{cases} -\frac{1}{2}\cos\Phi_0 J_0\left(\frac{1}{2}\Phi_{pp}\right) & n = 0 \\ \sin\Phi_0 J_n\left(\frac{1}{2}\Phi_{pp}\right) & n = 1;3;5\ldots \\ -\cos\Phi_0 J_n\left(\frac{1}{2}\Phi_{pp}\right) & n = 2;4;6\ldots \end{cases} \tag{3}$$

where A_n is the coefficient of the harmonic n and J_n is the Bessel function of order n. The characteristics of J_n make this spectrum to vanish sharply when $n > \Phi_{pp}/2$. Another interesting characteristic is that the spectrum can be regarded as quasicontinuous for large values of Φ_{pp} and that the envelope is rather flat for $n < 3\Phi_{pp}/8$. Fig. 2 gives an example where $\Phi_{pp} = 40\,000$ rad and $\Omega = 20$ kHz. Thus, the envelope of A_n vanishes for $n\Omega > 400$ MHz and it is fairly flat up to 300 MHz.

After this analysis we can conclude that the key to modulate the light at high frequencies is to drive large Φ_{pp}.

III. Experimental Arrangement

The results that we give in this paper have been obtained using two interferometers, both with the scheme shown in Fig. 1. One is set up with a HeNe laser, 633 nm, and about 45 m of singlemode fiber wound round the piezoelectric tube,

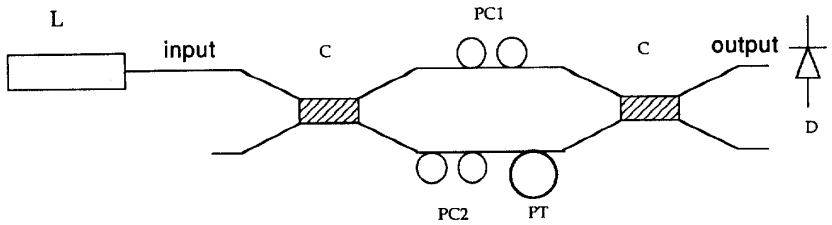

Fig. 1. Diagram of the experimental arrangement. L: laser, C: 3 db optical fiber coupler, PC1 and PC2: polarization controllers, PT: piezoelectric tube, D: detector.

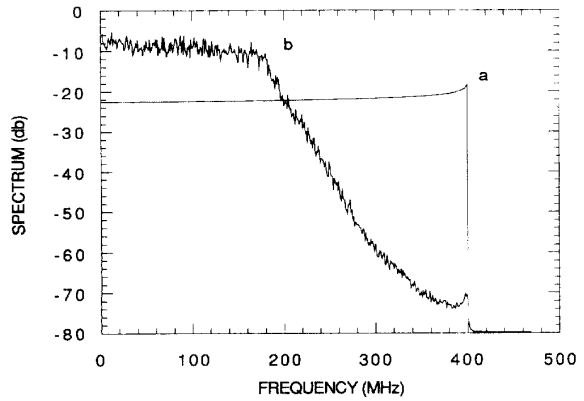

Fig. 2. (a) Frequency spectrum envelope calculated for $\Phi_{pp} = 40\,000$ rad and $\Omega = 20$ kHz. (b) Experimental spectrum obtained with a 125 MHz detector.

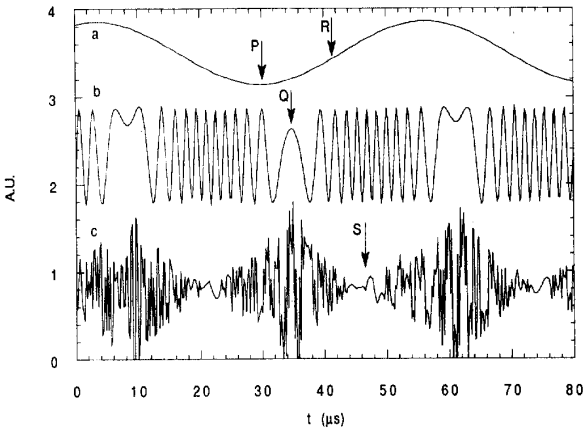

Fig. 3. Digitizing oscilloscope outputs. (a) Voltage applied to the piezoelectric tube. (b) Interferometer output (applied voltage: 80 mV_{pp}). (c) Detector output showing up a limited bandwidth (applied voltage: 16 V_{pp}).

while the other interferometer is set up with a diode laser, 830 nm, and winding 100 m of fiber. Both interferometers have been adjusted to minimize the path difference at equilibrium. This is particularly important for the second interferometer powered by the diode laser.

The piezoeletric tube, manufactured by Vernitron (PZT-5H, Ref.: 32-32200), has a length of 50.8 mm, an outside diameter of 50.8 mm and a wall thickness of 5.08 mm. The fundamental mechanical resonance is about 20 kHz and the Q is about 70, both measured with the fiber wound round the tube.

In order to generate a large phase modulation, i.e., large Φ_{pp}, we drive the piezoelectric tube with an amplifier that provides a maximum peak to peak voltage of about 250 V_{pp} and we tune the frequency Ω to match the fundamental mechanical resonance of the tube.

Our interferometers include two polarization controllers [8], although a standard application of an optical fiber Mach-Zender interferometer would require only one (e.g., PC1 in Fig. 1) to insure a good matching of the polarization states of the interfering beams. In fact, it is enough to use one polarization controller when we deal with small phase swings, but the characteristics of our phase modulator makes essential to include another controller before the modulator to deal with large phase swings.

Our phase modulator is formed by coiling a length of fiber onto a piezoelectric tube. This produces a linear birefringence and, when an AC voltage is applied, the birefringence will be modulated due to the modulated tension generated by the piezoelectric tube [9]. Thus, the modulator can be described by a dynamic Jones matrix whose eigenstates are constant, although its eigenvalues depend on the instantaneous tension. The function of the polarization controller PC2 of Fig. 1 is to adjust the polarization state at the entrance of the fiber coil to match one of its eigenstates. This insures that the polarization state is stationary at the output of the fiber coil and, therefore, the polarization controller PC1 can, effectively, perform its original function.

Fig. 3 gives an example of the interferometer output (830 nm) when a small phase swing is driven. The voltage applied to the piezoelectric tube was 80 mV_{pp} and the frequency $\Omega = 18.940$ kHz. The generated phase swing was 22π rad. The delay between points P and Q (Fig. 3) are due to the intrinsic characteristics of the mechanical resonance of the tube.

Fig. 4 shows the interferometer outputs before and after adjusting the polarization controller PC2. It is the same interferometer than in Fig. 3, but now 4 V_{pp} were applied. The number of cycles, as well as the phase swing, is about 50 times larger than in Fig. 3(b) and the resolution of the digitizing oscilloscope is not enough to record accurately the finer structure of the signal. However, the envelope is the key characteristic in this figure, since it relates to dynamic polarization changes. Before adjusting the polarization controller PC2 the envelope is a sort of amplitude modulation of frequency Ω. Looking at the oscilloscope screen one can adjust PC2 to get a flat envelope. At that moment we achieve a stationary polarization state at the output of the fiber coil. Finally, the controller PC1

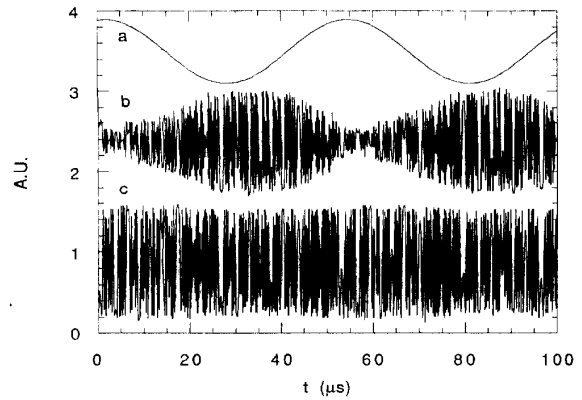

Fig. 4. Digitizing oscilloscope outputs. (a) Voltage applied to the piezoelectric tube (4 V_{pp}); (b) Interferometer output before adjusting PC2; (c) Interferometer output after adjusting PC2.

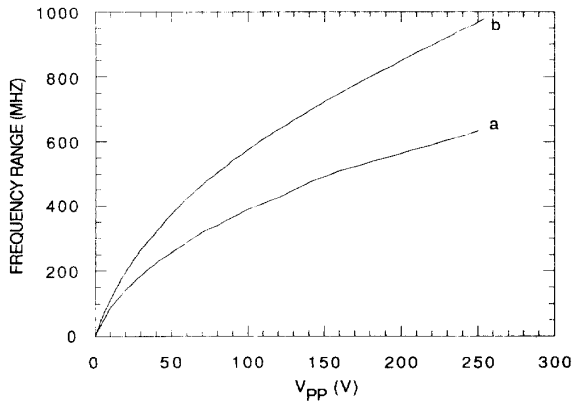

Fig. 5. Frequency range as a function of the peak to peak amplitude of the applied voltage. (a) 633 nm interferometer (fiber coil of 45 m); (b) 830 nm interferometer (fiber coil of 100 m).

can be adjust to maximize the amplitude of the output signal, to get a visibility as close as possible to 100%.

Once the polarization controllers have been adjusted, a further increase of the voltage applied to the piezoelectric tube gives rise to the output shown in Fig. 3(c). Now the envelope relates to the detector bandwidth and can be described as a 2 Ω amplitude modulation of the interferometer output. The regions where the signal exhibits smaller amplitudes (point S in Fig. 3) correspond to the regions of maximum slope of the applied voltage (point R), i.e., maximum frequency modulation and maximum phase change velocity.

Using a spectrum analyzer, it is straightforward to observe spectra similar to the theoretical example given in Fig. 2. These spectra allow for measuring the frequency range that our RF optical modulator is covering. Fig. 5 gives the frequency range that our interferometers cover as a function of the voltage applied to the piezoelectric tube. This figure shows that our modulating technique can cover frequencies up to 1 GHz at the present stage.

Finally, we give in Fig. 2(b) an example of the use of our RF modulation technique to calibrate the frequency response of a detector with a nominal 125 MHz bandwidth. We show in Fig. 2(b) the averaged spectrum. If we compare it with the theoretical spectrum envelope, Fig. 2(a), we can recognize the characteristic peak at 400 MHz, but attenuated by the response of the detector at such high frequencies. Since the theoretical spectrum is fairly flat up to 250 MHz, we can take this part of the experimental spectrum as a direct measurement of the frequency response of the detector. However, a more accurate measurement should be obtained dividing the experimental spectrum by the theoretical envelope.

IV. Conclusion

In this paper we demonstrate that an all-fiber Mach-Zender interferometer can be designed to generate RF modulated light. This optical output can be used to calibrate the frequency response of optical detectors. The simplicity of the technique is its main characteristic.

The present arrangements cover the frequency range 1 kHz–1 GHz, but the technique can be extended to higher frequencies, increasing the length of fiber wound round the piezoelectric tube and the amplitude of the applied voltage. The technique can be extended, as well, to shorter and larger wavelengths than 633 nm and 830 nm.

References

[1] M. V. Andres, "A novel optical fiber technique to calibrate the frequency response of optical detectors," *Meas. Sci. Technol.*, vol. 3, pp. 217–221, 1992.

[2] S. P. Robinson, D. R. Bacon, and B. C. Moss, "The measurement of the frequency response of a photodiode and amplifier using an opto-mechanical frequency response calibrator," *Meas. Sci. Technol.*, vol. 1, pp. 1184–1187, 1990.

[3] S. Kawanishi, A. Takada, and M. Saruwatari, "Wide-band frequency-response measurement of optical receivers using optical heterodyne detection," *J. Lightwave Technol.*, vol. 7, pp. 92–98, 1989.

[4] E. Eichen, J. Schlafer, W. Rideout, and J. Mccabe, "Wide-bandwidth receiver/photodetector frequency response measurements using amplified spontaneous emission from a semiconductor optical amplifier," *J. Lightwave Technol.*, vol. 8, pp. 912–916, 1990.

[5] D. M. Baney, W. V. Sorin, and S. A. Newton, "High-frequency photodiode characterisation using a filtered intensity noise technique," *IEEE Photon. Technol. Lett.*, vol. 6, pp. 1258–1260, 1994.

[6] C. A. Burrus, J. E. Bowers, and R. S. Tucker, "Improved very-high-speed packaged InGaAs *p-i-n* punch-through photodiode," *Electron. Lett.*, vol. 21, pp. 262–263, 1985.

[7] M. Abramowitz and I. A. Stegun, *Handbook of Mathematical Functions*. New York: Dover, 1972.

[8] H. C. Lefevre, "Single mode fractional wave device and polarization controllers," *Electron. Lett.*, vol. 16, pp. 778–80, 1980.

[9] S. C. Rashleigh and R. Ulrich, "High birefringence in tension-coiled single-mode fibers," *Optics Lett.*, vol. 5, pp. 354–356, 1980.

Jose L. Cruz, photograph and biography not available at the time of publication.

Javier Marzal, photograph and biography not available at the time of publication.

Miguel V. Andrés, photograph and biography not available at the time of publication.